Evaluating the surface temperature and vegetation index (*Ts/VI*) method for estimating surface soil moisture in heterogeneous regions

Zhaofei Liu, Zhijun Yao and Rui Wang

ABSTRACT

The surface temperature and vegetation index (*Ts/VI*) method is a remote sensing-based quantitative approach. It is widely used for estimating the evapotranspiration, evaporative fraction, and surface soil moisture (*SSM*). However, this method can only be used in flat regions. In this study, we investigated the effect of altitude when using the *Ts/VI* method for estimating the *SSM* in heterogeneous regions. The results showed that the temperature vegetation dryness index (TVDI) method performed poorly at estimating the *SSM* in the source region of the Yangtze River; there was a weak correlation with the observed *SSM*, and R^2 was only 0.167. However, the performance of the method improved considerably when the effects of both altitude and frozen soil were considered; the TVDI had a strong correlation with the observed *SSM*, and R^2 improved to 0.617. In the study area, the effects of altitude on the TVDI values were greater than those of the frozen soil. In general, the *Ts/VI* method can obtain satisfactory results in mountainous regions if the effects of both the altitude and frozen soil are considered.

Key words | MODIS, Qinghai-Tibetan Plateau, remote sensing retrieval, surface soil moisture, surface temperature, temperature vegetation dryness index

Zhaofei Liu
Zhijun Yao (corresponding author)
Rui Wang
Institute of Geographic Sciences and Natural Resources Research, Chinese Academy of Sciences,
Beijing 100101,
China
E-mail: *yaozj@igsnrr.ac.cn*

INTRODUCTION

Remote sensing has been used to determine surface turbulent energy fluxes and surface soil moisture (*SSM*) since the 1970s (Carlson 2007). The main advantage of remote sensing is that it provides spatially heterogeneous data because surface variables with spatial information are essential for several applications such as drought monitoring, scheduling irrigation, soil erosion mitigation, evaluating evapotranspiration, and forest management. Direct measurement is the most accurate method for estimating these variables, but this technique only provides point measurements. Thus, ground instruments are usually capable of only providing localized estimates of surface variables over large areas. Therefore, the *in situ* measurements obtained may not represent the spatial distribution of these variables at regional and global scales.

Many satellite-based techniques can be used for estimating the *SSM*. They can be classified as microwave and optical-thermal techniques. Passive microwave sensors have fine temporal resolution (1–1.5 passes per day) but coarse spatial resolution (~30 km). Specific methods based on active and passive microwave remote sensing were described by Wagner *et al.* (1999). Previous soil moisture mapping missions have included SMOS (Kerr *et al.* 2001), TMI (Bindlish *et al.* 2003), AMSR-E (Njoku *et al.* 2003), and SSM/I (Wentz 1997). However, their low spatial resolution makes it difficult to study sub-pixel variations at small scales. Optical-thermal remote sensing data can provide information at finer spatial resolution and remotely sensed thermal inertia has been employed for mapping soil moisture. The relationship between soil thermal inertia

doi: 10.2166/nh.2017.079

and water content can be used to estimate soil moisture (Lu *et al.* 2009), but many measurements are required in this method. Therefore, it is more feasible to use the apparent thermal inertia (Stisen *et al.* 2008) based on the noon–night land surface temperature (*LST*) difference to estimate *SSM*. However, this technique has limitations due to variable cloud cover conditions during the day and night or in two different hours during the daytime. Also, this method is not very accurate or reliable when surface vegetation cover is large (Petropoulos *et al.* 2015).

The surface temperature and vegetation index (*Ts/VI*) method is a synergistic approach for estimating surface turbulent energy fluxes and *SSM* conditions, and as the name suggests, it is based on information derived from the 'scatter plot' relationships between the satellite-derived vegetation index (*VI*) and surface temperature (*Ts*) measurements (Petropoulos *et al.* 2015). This method has been used in various applications, such as estimating evapotranspiration, evaporative fraction, and *SSM*, using the Advanced Very High Resolution Radiometer, Landsat, or Moderate Resolution Imaging Spectroradiometer (MODIS) sensors. The *Ts/VI* method assumes that the *SSM* has a complex relationship with the *Ts* and vegetation. This relationship was employed initially to detect canopy water stress and crop evapotranspiration using aerial thermal scanners (Heilman *et al.* 1976). Subsequently, based on remote thermal sensing imagery, indices such as the crop water stress index (CWSI) were developed for use in irrigation management (Jackson *et al.* 1981). The application of the *Ts/VI* method for *SSM* estimation was proposed by Nemani *et al.* (1993), who found a strong negative relationship between *Ts* and the normalized difference vegetation index (*NDVI*) for all biome types studied. The authors noted a distinct change in the slope between dry and wet days. The method was developed further by Moran *et al.* (1994) and Jiang & Islam (2001), and it is also called the triangle method or trapezoid method. Previous studies have focused mainly on the direct estimation of the *SSM* based on the *Ts/VI* space.

The basic assumption of the *Ts/VI* method is that *Ts*, which is associated with surface turbulent energy fluxes, is highly dependent on the *SSM*; the method is based on an interpretation of the image distribution in the *Ts/VI* space. In general, the range of *Ts* decreases as the vegetation cover increases. For a given *VI*, *Ts* increases gradually due to water stress in the surface soil from the minimum value at the wet edge (also called the cold edge) to the maximum value at the dry edge (also called the warm edge). On the other hand, the soil moisture decreases from the wet edge to the dry edge. Sandholt *et al.* (2002) proposed a simplified land surface dryness index called the temperature vegetation dryness index (TVDI), which is based on an empirical parameterization of the *Ts–VI* space. The results indicate that the spatial pattern of the TVDI is closely related to the *SSM* simulated using the MIKE SHE model. The TVDI may be estimated easily for each pixel without any ancillary data, and thus, it has been used widely for monitoring soil moisture conditions (Mallick *et al.* 2009; Gao *et al.* 2011; Son *et al.* 2012; He *et al.* 2013; Holzman *et al.* 2014; Zhang *et al.* 2014). The results of these past studies indicate that the TVDI has acceptable correlations with the observed soil moisture data. Thus, the TVDI is a useful index for monitoring the soil surface moisture condition. In addition, Son *et al.* (2012) compared the TVDI with a commonly used drought index called the CWSI, and the results showed that the TVDI is more sensitive to soil moisture stress than the CWSI. Comprehensive reviews of the application of remote sensing methods to the estimation of surface evapotranspiration and *SSM*, including their principles, advantages, and constraints, were conducted by Moran *et al.* (2004), Carlson (2007), Sun *et al.* (2012), and Petropoulos *et al.* (2015).

When applying the *Ts/VI* method, it is assumed that soil moisture is the main source of variation in the surface soil temperature, but this is only true for regions with flat terrain. Therefore, the most severe limitation of this method is that it requires a flat surface (Carlson 2007). Rahimzadeh-Bajgiran *et al.* (2012) incorporated observed air temperature calibrated using a digital elevation model (DEM) to account for a lapse rate while calculating the TVDI. However, the surface soil temperature is also affected by the altitude in heterogeneous regions. Therefore, the effect of altitude on the surface soil temperature needs to be considered when using the *Ts/VI* method to estimate surface turbulent energy fluxes or the *SSM*. However, the effect of altitude on the surface soil temperature has rarely been considered in most applications of the *Ts/VI* method. Thus, the main objective of this study was to evaluate the applicability of the *Ts/VI* remote sensing-based method for estimating the *SSM* in heterogeneous regions.

MATERIALS AND METHODS

First, a high mountain region was selected as the study area. The *Ts* data were then normalized to a certain altitude to consider the effect of the altitude on the *Ts*. Instead of the initial *Ts* data, the normalized *Ts–NDVI* scatter plot was used to detect the TVDI values. The TVDI values were obtained from remotely sensed land *Ts* and *NDVI* data. In addition, a semi-automated algorithm was developed for determining the dry and wet edges in the TVDI method. Finally, field observations of *SSM* data for a complete hydrological year were used to evaluate the performance of the TVDI method for *SSM* estimation.

TVDI method

The TVDI is an index for representing the *SSM* conditions. A simplified representation of the TVDI concept is presented in Figure 1. The *NDVI* and *LST* represent the vegetation and *SSM* conditions, respectively. The triangle is characterized by two physical limits, which denote the extreme conditions of *SSM* and evapotranspiration. The dry edge represents the limits of the *SSM* and evapotranspiration for different *VI* classes, and the lower horizontal wet edge indicates the maximum soil wetness and potential evapotranspiration (Sandholt *et al.* 2002).

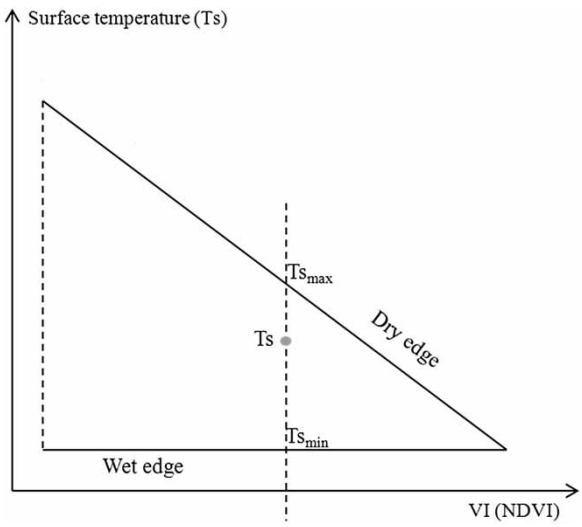

Figure 1 | Schematic illustration of the TVDI method (adapted from Sandholt *et al.* 2002).

The TVDI is estimated using the following equation (Sandholt *et al.* 2002):

$$\mathrm{TVDI} = \frac{Ts - Ts_{min}}{Ts_{max} - Ts_{min}} \tag{1}$$

$$Ts_{max} = a \times NDVI + b, \tag{2}$$

where *Ts* is the observed surface temperature (K or °C) at a given pixel. Ts_{min} is the minimum surface temperature observation for a given *NDVI*, which defines the wet edge; Ts_{max} is the maximum surface temperature observation for a given *NDVI*; and 'a' and 'b' define the dry edge based on a linear fit to the data. The TVDI ranges from 0.0 to 1.0.

Identification of the dry and wet edges

Identifying the dry and wet edges is essential for the TVDI method. In this study, we propose a semi-automated algorithm for determining the dry and wet edges based on scatter plots of the *Ts* and *NDVI*. This algorithm is based on previous studies by Tang *et al.* (2010) and Tomás *et al.* (2014). An important feature of the algorithm presented in this study is that it can automatically filter outliers. The steps followed to identify the dry edge are listed below:

1. Images with sufficient pixel values for the *Ts* and *NDVI* are selected. In this study, the number of pixels used was ≥10,000.
2. The *NDVI* is binned based on its data range. The bin size used in this study was 0.01. Bins with sufficient pixel values (≥100) are then selected.
3. In each bin, the maximum/minimum five *Ts* values are extracted and recorded as $mx_1, mx_2, \ldots, mx_5$. The difference in $mx_i - mx_{i+1}$ ($i = 1, 2, \ldots, 4$) is recorded as D_i. If $|2D_i| > |mx_1 - mx_5|$, then the maximum values $\geq mx_i$ (or the minimum values $\leq mx_i$) are deleted. The optimal maximum/minimum *Ts* for each bin in the *NDVI* is then extracted.
4. If an inflection point exists in the scatter plot of the maximum *Ts* and *NDVI* (Figure 2), it is identified visually. The scatter points located to the right-hand side of the inflection point are selected for estimating the dry edge using least squares regression; otherwise, the dry edge is estimated by a least squares regression of the maximum *Ts* in each bin.

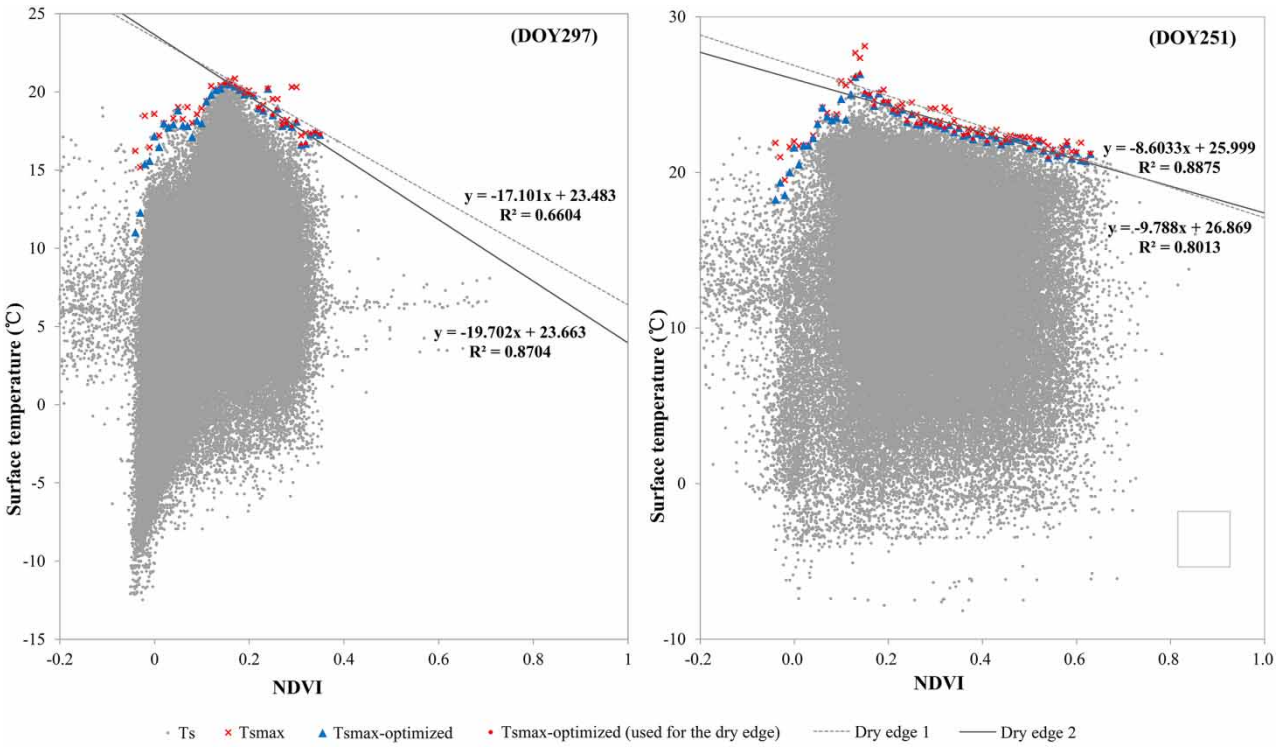

Figure 2 | Schematic diagram illustrating the optimized dry edge.

The wet edge is identified by averaging the minimum *Ts* values in each bin.

Considering the effect of altitude on the *LST*

The surface temperature axis shown in Figure 1 is a simplified term based on the difference between the surface temperature and air temperature (*Ts* – *Ta*). It represents the energy exchange at the Earth's surface (Jackson *et al.* 1981). In general, *Ts* – *Ta* is often replaced by *Ts* due to the lack of air temperature data, because grid *Ta* data are difficult to obtain over large areas, whereas grid *Ts* data can be obtained easily from remote sensing images. The surface temperature is considerably affected by the heterogeneity of the Earth's surface, especially the heterogeneous altitude, which is usually assumed to decrease in a linear manner with the elevation according to a lapse rate (rate of decrease in the surface temperature with elevation). Therefore, the effect of altitude on the *LST* (lapse rate) should be considered in a quantitative manner when using remotely sensed *Ts* data (Wan & Dozier 1996; Minder *et al.* 2010). Otherwise, the *Ts*/*VI* method is only suitable for small regions and regions with little topographic variation.

The study area is the source region of the Yangtze River (SRYR), which is located in the central–eastern part of the Qinghai–Tibetan Plateau, China (Figure 3). This region includes a major river basin located at a very high altitude. The natural environment and ecosystem are highly sensitive to the availability of water. The study area is located in a mountainous region, and thus the lapse rate of 4.6 °C/km for the Cascade Mountains recommended by Minder *et al.* (2010) was used in this study. The DEM employed was derived from the ASTER (Advanced Spaceborne Thermal Emission and Reflection Radiometer) GDEM2 (Global Digital Elevation Model Version 2), a product created by the Ministry of Economy, Trade, and Industry (METI) in Japan and the National Aeronautics and Space Administration (NASA) in the United States. Its spatial resolution is approximately 30 m. The data were resampled to 1,000 m to match the resolution of the MODIS products. The altitude ranged from 4,413 m above sea level (a.s.l.) to 6,571 m a.s.l., and the average altitude was 4,963 m a.s.l.

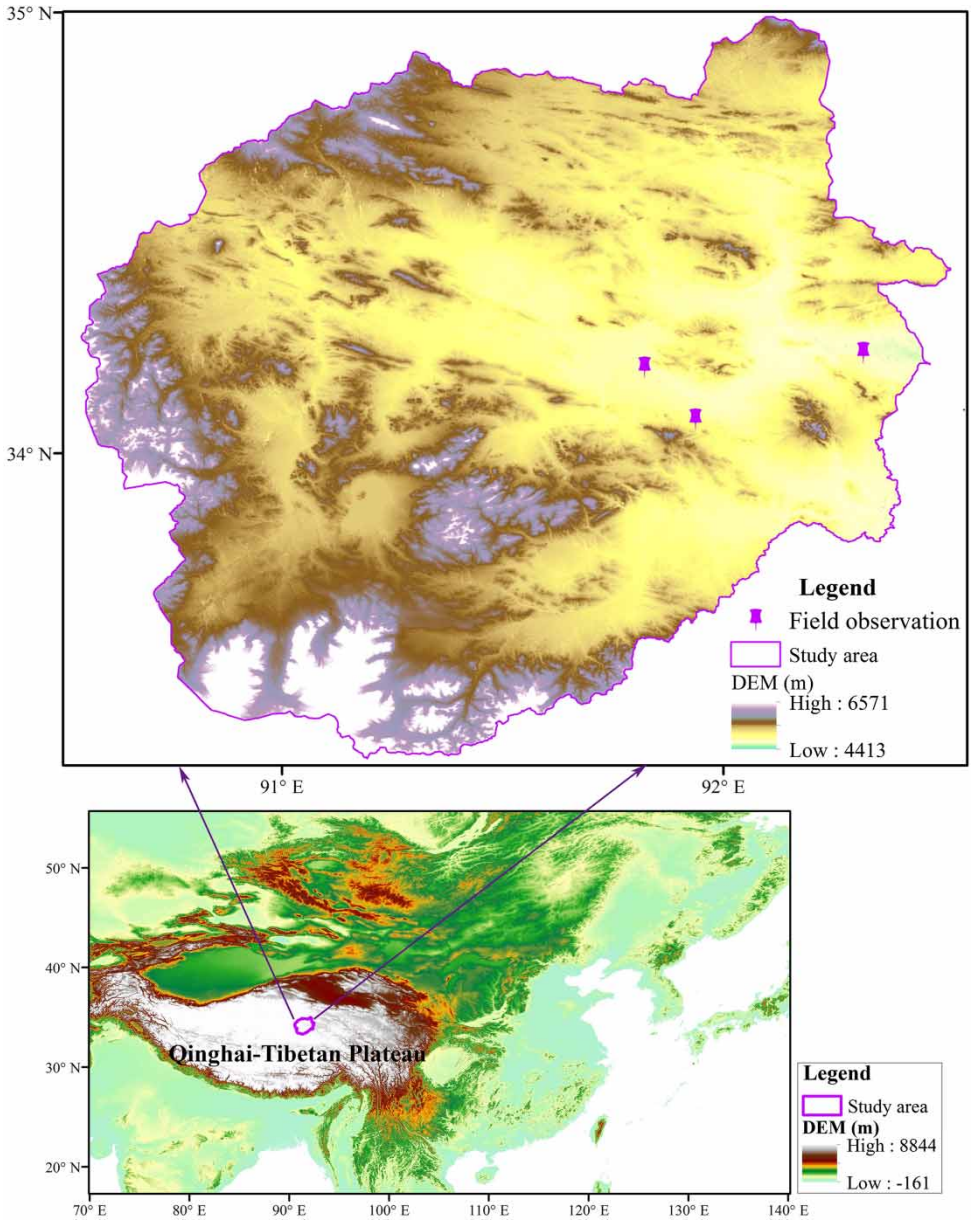

Figure 3 | Locations of the study area and field observation sites.

Most of the pixels (98.4%) were located between 4,500 m a.s.l. and 5,500 m a.s.l.

Remote sensing data

In this study, the MODIS LST product MOD11A1 and NDVI product MOD13A2 were used for *Ts* and *VI*, respectively. These products were obtained from NASA's Earth Observing System Data and Information System (http://reverb.echo.nasa.gov/reverb). MOD11A1 is produced daily at a spatial resolution of 1 km, whereas MOD13A2 is generated every 16 days at a spatial resolution of 1 km. The MODIS products were originally stored as a sinusoidal projection with a nominal spatial resolution of 1 km. The MODIS Reprojection Tool was used to reproject the images onto geographic latitude/longitude coordinates (Datum WGS-84). The MOD11A1 *Ts* data were normalized by considering the effects of altitude. Thus, each pixel's *Ts*

value was interpolated to the lowest altitude in the image using the DEM, where the assumed lapse rate was 4.6 °C/km. As mentioned above, we assumed that the surface soil temperature was affected mainly by *SSM* when we applied the *Ts/VI* method. As normalizing the *Ts* data can remove the effect of altitude on *Ts* that exists in heterogeneous regions, we used the normalized *Ts* data to estimate the TVDI values based on the normalized *Ts–NDVI* scatter plot.

Field observations of *SSM*

A field survey was conducted to obtain *SSM* data from 15 June 2014 to 30 June 2015. This study period included a complete hydrological year with low, normal, and high *SSM* contents, thereby allowing us to test the method over a wide range of soil wetness conditions. Measurements were obtained at four sites, but the instrument at one site was eventually damaged by natural environmental conditions. Therefore, the observed *SSM* data were acquired from only three sites (Figure 3). At each site, the soil moisture content and temperature were determined at two depths (10 and 60 cm), and the data were recorded by an Onset soil moisture and temperature sensor. This soil moisture and temperature measurement device could determine the volumetric soil moisture content and temperature with accuracies of 1% and 0.2 °C, respectively. The observation time step was 1 hour. Finally, the TVDI values were compared with field observed *SSM* data.

RESULTS

Normalized *Ts–NDVI* scatter plots

The normalized *Ts* data were used to remove the effect of altitude on the surface temperature, thereby satisfying the assumption of the *Ts/VI* method. Daily normalized *Ts–NDVI* scatter plots were created from 15 June 2014 to 30 June 2015. The dry and wet edges were determined from each normalized *Ts–NDVI* scatter plot to obtain the TVDI. Figure 4 illustrates some examples of the scatter plots of the normalized *Ts–NDVI* space. The pixels in each plot form a triangle denoting the wide range of soil moisture contents in the study area. The observations were consistent with the suggestion of Sandholt *et al.* (2002), namely, that the *Ts* decreases as the *NDVI* increases. The dry edges were identified by least squares regression, as described in the section 'Identification of the dry and wet edges', and there were significant correlations ($R^2 > 0.8$) in all cases. However, it should be noted that the observed surface soil temperature at all three field sites was below 0 °C from 27 October 2014 to 12 April 2015 (Figure 5), that is, the surface soil was frozen during this period. As mentioned above, the theoretical basis of the *Ts/VI* method is that the surface soil temperature is highly dependent on *SSM*, but this theoretical basis is not suitable for frozen ground. Therefore, the normalized *Ts–NDVI* scatter plots obtained during this frozen period were not suitable for determining the TVDI values, as discussed later.

The dry edges are shown for each scatter plot in Figure 4. The large area (13.5×10^4 km^2) contained sufficient pixels to represent the soil moisture and vegetation cover, as required by the TVDI method. The wide ranges of the *NDVI* and *Ts* data are evident in all the scatter plots, where the maximum *NDVI* of 0.8 occurred in August (i.e., 14 August 2014, DOY226) and the maximum *Ts* of 45 °C occurred in July (i.e., 15 July 2014, DOY196). Thus, in the SRYR, the vegetation cover was highest in August, and the surface temperature was greatest in July, which is consistent with the local water conditions (*SSM*) and incoming solar radiation, respectively.

The different characteristics of the dry edge parameters can indicate the availability of soil water. The results showed that the *LST* had a relatively narrow dynamic range in the summer months, for example, on 1 July (DOY182), 15 July (DOY196), 31 July (DOY212), 14 August (DOY226), and 6 September (DOY249) in 2014, as shown by the relatively flat dry edge slope and low intercept in Figure 4. This figure indicates the high availability of soil moisture, elevated evapotranspiration, and relative homogeneity of the *LST*. In other months, the situation was reversed, indicating the low availability of soil moisture (e.g., on 16 June 2014 (DOY167), 25 October 2014 (DOY298), 20 April 2015 (DOY110), 6 May 2015 (DOY126), 27 May 2015 (DOY147), and 6 June 2015 (DOY157)). In addition, there was a low slope and the *Ts* increased near the bare soil with precipitation. In general, the dry edge parameters obtained from the normalized *Ts–NDVI* scatter plots clearly

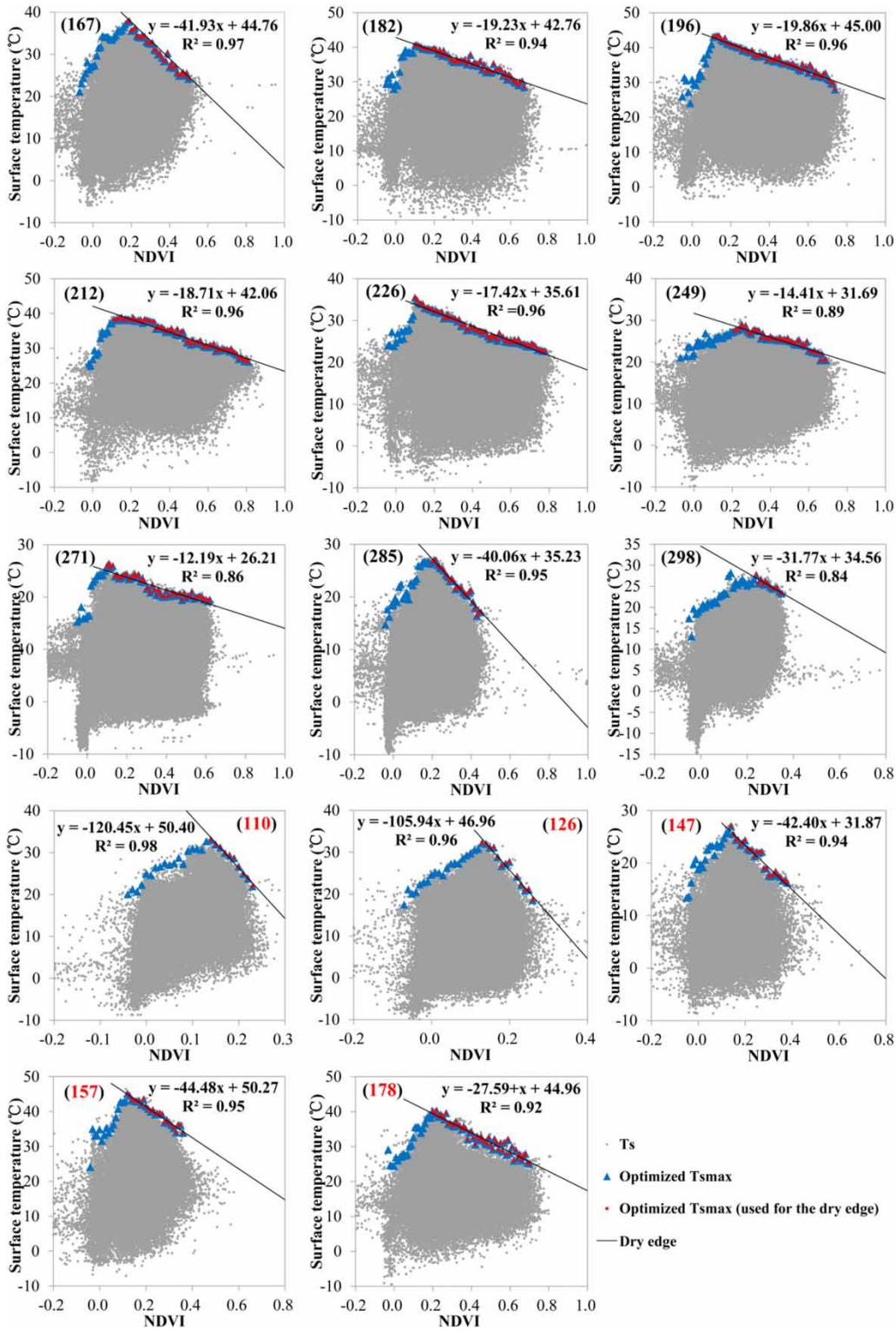

Figure 4 | Normalized *Ts–NDVI* scatter plots and dry edges. The triangle denotes the optimized maximum *Ts* in each bin of the *NDVI*. The dot is the optimized maximum *Ts* used for dry edge extraction. The line indicates the dry edge. The first nine plots are observations during 2014, while the last five plots are observations during 2015.

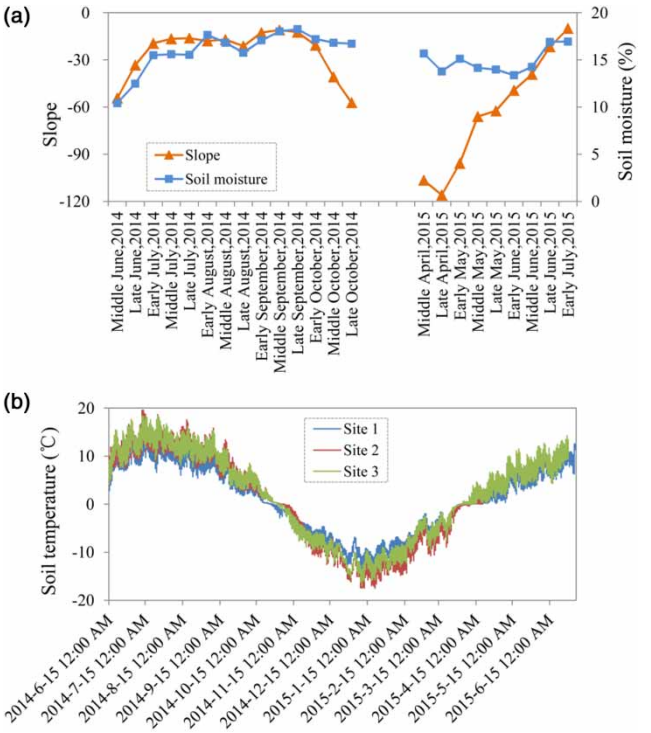

Figure 5 | Temporal variations in (a) mean slope of the dry edge and observed soil moisture over 10 days and (b) hourly observed surface soil temperature at the three field sites.

indicated the surface wetness, and the results were consistent with the findings of previous studies (Mallick *et al.* 2009; Son *et al.* 2012; Sun *et al.* 2012).

In general, there was a strong correlation between the slope of the dry edge and the availability of surface soil water. The temporal variations in the mean slope and observed *SSM* over 10 days during the observation period (from the middle of June 2014 to early July 2015) are shown in Figure 5. The hourly observed surface soil temperatures at the three field sites are also shown in this figure. The annual mean surface soil temperature in SRYR was 1.0 °C. The mean surface soil temperature was highest in July (12.7 °C) and lowest in January (−12.3 °C). The surface soil temperatures at the three field sites were lower than 0 °C between 27 October 2014 and 12 April 2015. The *SSM* observed at the three field sites ranged from 10% to 20%.

Figure 5(a) shows a strong correlation between the mean slope of the dry edge and the observed *SSM* over 10 days in SRYR. The correlation coefficient for the whole period was 0.568. However, the correlation between the mean slope and observed *SSM* was weak during the period from the middle of October 2014 until late May 2015, possibly because the surface soil could have been frozen in some regions. The surface soil temperatures at the three observation sites exceeded 0 °C. Thus, the temperature may have been below 0 °C in other regions of the SRYR because the topography and underlying surface are complex in this region. The theoretical basis of the *Ts/VI* method is invalid for a frozen soil surface as the surface soil temperature is not dependent on the *SSM* because of the effect of the frozen ground. The range of the *NDVI* was relatively narrow during this period (Figure 4), and it was used for the dry edge extraction, which might also explain these results. Therefore, the *Ts–NDVI* scatter plots produced during this period were not suitable for detecting the *SSM*. When this frozen period was not included, the correlation between the slope and *SSM* was stronger; the correlation coefficient between the mean slope and observed *SSM* over 10 days was 0.820.

Comparison of the TVDI and observed *SSM*

The TVDI values were compared with the observed *SSM* values in order to determine their correlation. The *Ts/VI* method is affected to a large extent by the altitude and frozen soil. Thus, Figure 6 shows scatter plots of the TVDI and observed *SSM* in four conditions with or without consideration of the effects of altitude and frozen soil. According to the soil temperature determined at the three field sites, frozen soil was also identified based on the correlation between the mean slope of the dry edges and the observed *SSM*, as shown in Figure 5(a). As mentioned above, the surface soil may have been frozen between October 2014 and late May 2015. Thus, this period was identified as a 'frozen soil period'. Figure 5 shows that the observed *SSM* ranged mainly between 10% and 20%, whereas the TVDI values were between 0.2 and 0.9. The TVDI had a weak correlation with the observed *SSM* when the effects of altitude and frozen soil were not considered (the R^2 value was only 0.167). However, the correlation between the TVDI and observed *SSM* was stronger when the effect of altitude or frozen soil was considered. Therefore, the effects of altitude and frozen soil should be taken into account when using the TVDI method. The correlation was stronger when considering

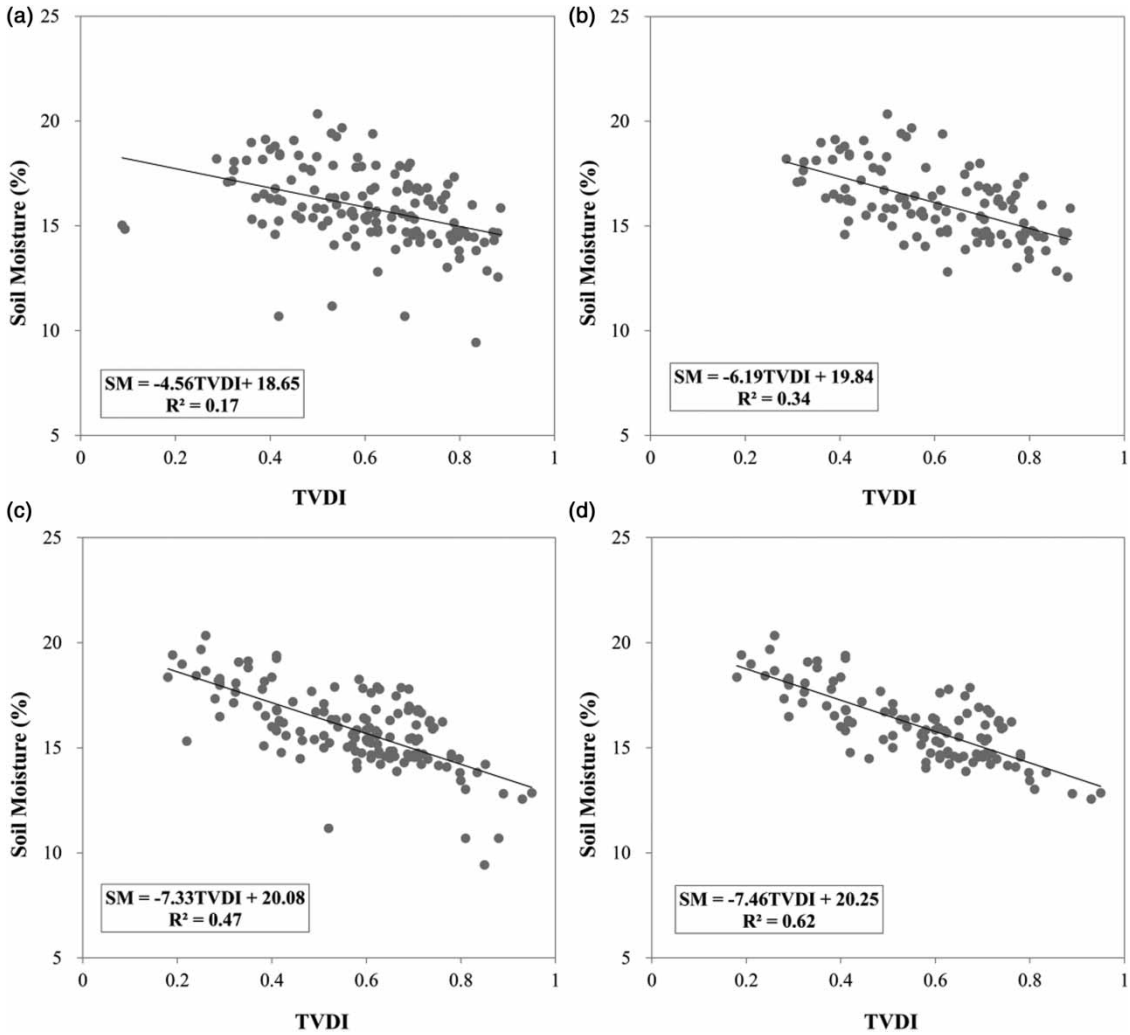

Figure 6 | Scatter plots of TVDI and observed *SSM* when: (a) not considering the effects of altitude or frozen soil; (b) considering the effect of frozen soil only; (c) considering the effect of altitude only; and (d) considering the effects of both altitude and frozen soil.

the effect of altitude rather than that of frozen soil. Thus, the effect of altitude on the TVDI ($R^2 = 0.474$) was greater than that of frozen soil ($R^2 = 0.343$). The TVDI had a relatively strong correlation with the observed *SSM* when the effects of both altitude and frozen soil were considered; in this case, R^2 improved to 0.617.

DISCUSSION AND CONCLUSION

The *Ts/VI* method is a remote sensing-based approach that is representative of field conditions. It is used widely for estimating the evapotranspiration, evaporative fraction, and *SSM*. It is assumed that the surface soil temperature is affected mainly by the *SSM* for a certain vegetation cover type, but this is only true over flat regions. The surface soil temperature is also influenced by altitude in heterogeneous regions, especially in areas with high mountains. This study considered the effect of altitude when using the *Ts/VI* method to estimate the *SSM* in a heterogeneous region, that is, the SRYR, which is located in a high mountainous region that is also home to one of the world's biggest river basins. The following conclusions can be made based on our results:

1. Identifying the dry and wet edges is essential when applying the TVDI method. Thus, in this study, we proposed a

semi-automated algorithm for determining the dry and wet edges based on a scatter plot of the *Ts* and *NDVI*. This algorithm is simple, practical, and effective. It is capable of rejecting anomalous points that might have negative effects on the identification of the dry edge. These anomalous points would reduce the accuracy of dry edge identification.

2. In general, the *Ts/VI* method assumes that surface soil temperature is affected mainly by *SSM* and vegetation cover. However, the surface soil temperature is also influenced by the altitude over heterogeneous regions. Therefore, the effect of altitude on the surface soil temperature needs to be considered when using the *Ts/VI* method for estimating surface turbulent energy fluxes and the *SSM*. In this study, we evaluated the performance of the Ts/VI method (TVDI) in estimating the *SSM* based on field observed data obtained over the high mountain region of the SRYR. The *Ts* data were normalized to a specific altitude to consider the effect of altitude on the *Ts*. The normalized *Ts–NDVI* scatter plots were then used instead of the initial *Ts* data to detect the dry and wet edges. The results showed that the TVDI had a weak correlation with the observed *SSM* when the effects of altitude and frozen soil were not considered (R^2 was only 0.167). The correlation between TVDI and the observed *SSM* was stronger when the effect of altitude was considered (R^2 improved to 0.474). Thus, we conclude that the effect of altitude should be considered when using the TVDI method to estimate the *SSM* in heterogeneous regions.
3. The effect of frozen soil also needs to be considered when employing the TVDI method to estimate the *SSM* in high altitude regions. The results of this study showed that the TVDI method is not suitable for estimating the *SSM* under conditions with frozen soil. The correlation between the TVDI and observed *SSM* improved when the effect of frozen soil was considered; R^2 improved from 0.167 to 0.343. Most of the applications of the remote sensing method for estimating the *SSM* involve agricultural drought monitoring, which focuses on the soil moisture during unfrozen periods of the year (spring, summer, and autumn). However, it should be noted that the TVDI values during the frozen period (usually winter) need to be rejected before establishing the relationship between the TVDI and observed *SSM*. This is because the TVDI values during the frozen period would reduce the correlation between the TVDI and observed *SSM*, thereby negatively affecting *SSM* estimation.
4. The traditional TVDI method performed poorly at estimating the *SSM* conditions in the SRYR. The TVDI had only a weak correlation with the observed *SSM* (R^2 of only 0.167). However, the performance of the method improved considerably when the effects of both altitude and frozen soil were considered. In this case, the TVDI had a strong correlation with the observed *SSM* (R^2 improved to 0.617). Therefore, we conclude that the *Ts/VI* method is suitable for obtaining satisfactory results in regions with high mountains if the effects of both altitude and frozen soil are considered.

ACKNOWLEDGEMENTS

This study was supported and funded by the National Natural Science Foundation of China (Grant Nos 41571027, 41371058, and 41190080). We also thank Lei Wang and Liguang Jiang for assistance in the field.

REFERENCES

Bindlish, R., Jackson, T. J., Wood, E., Huilin, G., Starks, P., Bosch, D. & Lakshmi, V. 2003 Soil moisture estimates from TRMM microwave imager observations over the Southern United States. *Remote Sensing of Environment* **85**, 507–515.

Carlson, T. 2007 An overview of the 'triangle method' for estimating surface evapotranspiration and soil moisture from satellite imagery. *Sensors* **7**, 1612–1629.

Gao, Z., Gao, W. & Chang, N. B. 2011 Integrating temperature vegetation dryness index (TVDI) and regional water stress index (RWSI) for drought assessment with the aid of LANDSAT TM/ETM+ images. *International Journal of Applied Earth Observation and Geoinformation* **13** (3), 495–503.

He, J., Yang, X. H., Huang, S. F., Di, C. L. & Mei, Y. 2013 Study on soil moisture by thermal infrared data. *Thermal Science* **17** (5), 1375–1381.

Heilman, J. L., Kanemasu, E. T., Rosenberg, N. J. & Blad, B. L. 1976 Thermal scanner measurement of canopy temperatures to estimate evapotranspiration. *Remote Sensing of Environment* **5**, 137–145.

Holzman, M. E., Rivasa, R. & Piccolo, M. C. 2014 Estimating soil moisture and the relationship with crop yield using surface temperature and vegetation index. *International Journal of Applied Earth Observation and Geoinformation* **28**, 181–192.

Jackson, R. D., Idso, S. B., Reginato, R. J. & Pinter, P. J. 1981 Canopy temperature as a crop water-stress indicator. *Water Resource Research* **17**, 1133–1138.

Jiang, L. & Islam, S. 2001 Estimation of surface evaporation map over Southern great plains using remote sensing data. *Water Resource Research* **37**, 329–340.

Kerr, Y. H., Waldteufel, P., Wigneron, J. P., Martinuzzi, J. M., Font, J. & Berger, M. 2001 Soil moisture retrieval from space: the soil moisture and ocean salinity (SMOS) mission. *IEEE Transactions on Geosciences and Remote Sensing* **39**, 1729–1735.

Lu, S., Ju, Z., Ren, T. & Horton, R. 2009 A general approach to estimate soil water content from thermal inertia. *Agricultural and Forest Meteorology* **149**, 1693–1698.

Mallick, K., Bhattacharya, B. K. & Patel, N. K. 2009 Estimating volumetric surface moisture content for cropped soils using a soil wetness index based on surface temperature and NDVI. *Agricultural and Forest Meteorology* **149**, 1327–1342.

Minder, J. R., Mote, P. W. & Lundquist, J. D. 2010 Surface temperature lapse rates over complex terrain: lessons from the cascade mountains. *Journal of Geophysical Research* **115**, D14122.

Moran, M. S., Clarke, T. R., Inoue, Y. & Vidal, A. 1994 Estimating crop water deficit using the relation between surface-air temperature and spectral vegetation index. *Remote Sensing of Environment* **49**, 246–263.

Moran, M. S., Peters-Lidard, C. D., Watts, J. M. & McElroy, S. 2004 Estimating soil moisture at the watershed scale with satellite-based radar and land surface models. *Canadian Journal of Remote Sensing* **30**, 805–826.

Nemani, R., Pierce, L. & Running, S. 1993 Developing satellite-derived estimates of surface moisture status. *Journal of Applied Meteorology* **32**, 548–557.

Njoku, E. G., Jackson, T. J., Lakshmi, V., Chan, T. K. & Nghiem, S. V. 2003 Soil moisture retrieval from AMSR-E. *IEEE Transactions on Geosciences and Remote Sensing* **41** (2), 215–229.

Petropoulos, G. P., Ireland, G. & Barrett, B. 2015 Surface soil moisture retrievals from remote sensing: current status, products & future trends. *Physics and Chemistry of the Earth* **83–84**, 36–56.

Rahimzadeh-Bajgiran, P., Omasa, K. & Shimizu, Y. 2012 Comparative evaluation of the vegetation dryness index (VDI), the temperature vegetation dryness index (TVDI) and the improved TVDI (iTVDI) for water stress detection in semi-arid regions of Iran. *ISPRS Journal of Photogrammetry and Remote Sensing* **68**, 1–12.

Sandholt, I., Rasmussen, K. & Andersen, J. 2002 A simple interpretation of the surface temperature/vegetation index space for assessment of surface moisture status. *Remote Sensing of Environment* **79**, 213–224.

Son, N. T., Chen, C. F., Chen, C. R., Chang, L. Y. & Minh, V. Q. 2012 Monitoring agricultural drought in the lower Mekong basin using MODIS NDVI and land surface temperature data. *International Journal of Applied Earth Observation and Geoinformation* **18**, 417–427.

Stisen, S., Sandholt, I., Nöörgard, A., Fensholt, R. & Jensen, K. H. 2008 Combining the method with thermal inertia to estimate regional evapotranspiration-applied to MSG-SEVIRI data in the Senegal River basin. *Remote Sensing of Environment* **112**, 1242–1255.

Sun, L., Sun, R., Li, X. W., Liang, S. L. & Zhang, R. H. 2012 Monitoring surface soil moisture status based on remotely sensed surface temperature and vegetation index information. *Agricultural and Forest Meteorology* **166/167**, 175–187.

Tang, R., Li, Z. L. & Tang, B. 2010 An application of the Ts–VI triangle method with enhanced edges determination for evapotranspiration estimation from MODIS data in arid and semi-arid regions: implementation and validation. *Remote Sensing of Environment* **114**, 540–551.

Tomás, A., Nieto, H., Guzinski, R., Salas, J., Sandholt, I. & Berliner, P. 2014 Validation and scale dependencies of the triangle method for the evaporative fraction estimation over heterogeneous areas. *Remote Sensing of Environment* **152**, 493–511.

Wagner, W., Lemoine, G. & Rott, H. 1999 A method for estimating soil moisture from ERS scatterometer and soil data. *Remote Sensing of Environment* **70**, 191–207.

Wan, Z. & Dozier, J. 1996 A generalized split-window algorithm for retrieving land-surface temperature from space. *IEEE Transactions on Geosciences and Remote Sensing* **34**, 892–905.

Wentz, F. J. 1997 A well-calibrated ocean algorithm for SSM/I. *Journal of Geophysical Research* **102** (C4), 8703–8718.

Zhang, F., Zhang, L. W., Shi, J. J. & Huang, J. F. 2014 Soil moisture monitoring based on land surface temperature vegetation index space derived from MODIS data. *Pedosphere* **24** (4), 450–460.

First received 25 April 2017; accepted in revised form 27 September 2017. Available online 8 November 2017